Morphobot: A Platform for Morphogenesis in Robot Swarm

Xiaoyang Qin, Yongliang Yang, *Member, IEEE*, Mengyun Pan, Long Cui, and Lianqing Liu, *Senior Member, IEEE*

***Abstract*—Various robot platforms have been developed for investigating new algorithms for swarm robotics. Morpho-genetic engineering in robot swarms, however, proposes new requirements for platforms: precise motion control, physical interactions with the environment or neighbor robots, and functionalized shells. Few current platforms fulfill all the above characteristics. Here, we present Morphobot, a robot platform for morphogenetic engineering in swarm robotics. Its direct current coreless motors provide physical support and strong power, meanwhile, these needle-like motors also enhance the physical interactions among robots. Each Morphobot has a changeable shell. It is functionalized for programming local interactions, through physical contact or communication, among Morphobots. We characterized the mobility of Morphobot to test its capability of moving and physically interacting with its neighbors. To demonstrate its advantages in the morphogenesis of robot swarms, we designed two morphogenetic engineering experiments. The results revealed that swarms of Morphobots can form patterns via physical interactions and optical communications.**

***Index Terms*—Multi-robot systems, swarm robotics, autonomous agents, morphogenetic engineering.**

I. Introduction

A SYSTEM of robot swarms emerges global behaviors via local interactions among robots. In this decentralized manner, the robot swarms can accomplish tasks beyond the capabilities of a single robot [1] and the systems are robust and scalable. Systems of robot swarms, thus, have great potential in various applications, such as search and rescue [2], area exploration [3], [4], [5], and navigation [6]. To execute tasks in most applications, a universal step is forming a proper morphology of the robot swarms.

Morphogenetic engineering translates the principles of morphogenesis in natural systems into robot swarms to form patterns in a self-organized manner [7]. Currently, many swarm intelligence algorithms are inspired by natural swarms, especially biological swarm systems. During embryo development and tissue regeneration, cell swarms dynamically create their own physical shapes, which is termed as morphogenesis [8]. It occurs in a distributed, self-organized, and emergent manner [7]. For example, cells in embryos interact with each other and with the micro-environment in the physical and chemical cues. These local interactions coordinate the movement of involved cells and emergently form the shapes of organs in embryos at a global level [8]. The morphogenesis in biology inspires new algorithms for morphogenetic engineering, which benefits tasks such as mapping, area exploration, and area coverage in robot swarms. Meanwhile, the robot swarms can also serve as an instrument to investigate the physical principles of morphogenesis in developmental and regenerative biology.

Though having many potentials, morphogenetic engineering presents new challenges for current research platforms of swarm robotics. The existing research platforms for swarm robots include Kilobots [9], GRITSBot [10], Jasmine [11], Alice [12], [13], e-puck [14], Colias IV [15], mROBerTO 2.0 [16], TinyTeRP [17], and AMiR [18]. Among them, Kilobots are classic research platforms for swarm robotics. Using Kilobot, Slavkov [7] and Hyondong [19] et al. investigated morphogenesis in robot swarms. In their experiments, an accidental phenomenon of "*robot loss*" existed, because a Kilobot moves by vibrating its three-pin legs and it cannot be precisely controlled. The mROBerTO 2.0 is a small-sized robot with wheels. It can control its motion precisely, as its step motors are capable of micro-stepping down to 1/32 of a full step [16]. Its wheels, however, make its motion can hardly be modified by the physical interactions between neighboring robots and the environment. Moreover, all the above platforms are unable or difficult to change their shells, which may serve as coding variables for programming robot swarms. Besides the platforms that have been used in morphogenetic engineering, other swarm robot platforms such as r-one [20], SwarmBot [21], Khepera IV, Pheeno [22], WolfBot [23], marXbot [24], and s-bot [25] all pursue the high performance of a single robot, which limits their scalability. Meanwhile, they all have more or less the same

Manuscript received 1 June 2023; accepted 12 September 2023. Date of publication 27 September 2023; date of current version 4 October 2023. This letter was recommended for publication by Associate Editor Z. Zhang and Editor X. Liu upon evaluation of the reviewers' comments. This work was supported in part by the National Natural Science Foundation of China under Grant 62273338 and in part by the Fundamental Research Program of SIA under Grant 2022JC3K01. *(Corresponding author: Yongliang Yang; Lianqing Liu.)*

Xiaoyang Qin and Mengyun Pan are with the State Key Laboratory of Robotics, Shenyang Institute of Automation, Chinese Academy of Sciences, Shenyang 110016, China, and with the Institutes for Robotics and Intelligent Manufacturing, Chinese Academy of Sciences, Shenyang 110169, China, and also with the University of Chinese Academy of Sciences, Beijing 100049, China (e-mail: qinxiaoyang@sia.cn; panmengyun@sia.cn).

Yongliang Yang, Long Cui, and Lianqing Liu are with the State Key Laboratory of Robotics, Shenyang Institute of Automation, Chinese Academy of Sciences, Shenyang 110016, China, and also with the Institutes for Robotics and Intelligent Manufacturing, Chinese Academy of Sciences, Shenyang 110169, China (e-mail: ylyang@sia.cn; cuilong@sia.cn; lqliu@sia.cn).

This letter has supplementary downloadable material available at https://doi.org/10.1109/LRA.2023.3320021, provided by the authors.

Digital Object Identifier 10.1109/LRA.2023.3320021

TABLE I
COMPARISON OF MULTI-ROBOT PLATFORMS

Robot	Year	Sensors	Locomotion	Size (cm)	Cost	Required Features			Scalability
						SAA[1]	CSM[2]	CS[3]	
Morphobot	2023	IR, 3D accel, 3D gyro, WIFI, bluetooth	pin rotation, 20cm/s	3.5	$35	●	●	●	charge, power
mROBerTO 2.0 [16]	2020	instance, aspect, bluetooth	wheel, 80mm/s	2.2	$140	●			none
Colias IV [15]	2018	instance, camera, mpu9520, bluetooth microphones	wheel, 25cm/s	4	$100	●		●	none
AMiR [18]	2015	IR, instance, aspect, ambient light	wheel, 14cm/s	6.5	$66	●			none
GRITSBot [10]	2015	distance, bearing, 3D accel, 3D gyro	wheel, 25cm/s	3	$50	●			charge, program, calibrate
Kilobots [9]	2013	distance, ambient light	vibration, 1cm/s	3.3	$14		●		charge, power, program
TinyTeRP [17]	2013	distance, microphones, 3D accel, 3D gyro	wheel, 50cm/s	2	$50	●			none
Jasmine [11]	2009	distance, bearing, light color	wheel, 50cm/s	3	$130	●			charge
e-puck [14]	2007	range, bearing, 3D accel, microphones	wheel, 13cm/s	7.5	$950	●		●	none
Alice [12], [13]	1998	distance, bearing, cliff	wheel, 2cm/s	2	N/A	●			none

[1] SAA: strong athletic ability
[2] CSM: changeable state of motion
[3] CS: changeable shape

problems mentioned earlier. Detailed comparisons are shown in Table I.

In summary, morphogenetic engineering proposes new requirements for swarm robotic platforms:

1) Precise motion control. In morphogenetic engineering, the robot swarms emerge into a final global pattern via local interactions among its robots. To test self-organized algorithms for morphogenetic engineering, the motion of each individual robot should mainly be affected by the interactions among robots with as little noise from the locomotion of robots as possible.
2) Facilitating interactions among robots. The local interaction drives the morphogenesis of robot swarms. To accelerate the process of morphogenesis and magnify the effects of local interactions, especially in a self-organized system, a robot in swarms needs to be sensitive to these external interactions. The state of robot individuals thus could be affected and the swarm eventually emerges into the pre-designed morphology.
3) Functional and changeable shells. The local interactions determine the final global morphology by affecting the state of each robot individual. The features of robot shells can serve as variables to code the interactions between robots. For example, the adhesion among robots can be digitalized via the arrangement of magnetic slides on the boundary of the shell. According to specific applications, different sensors could be mounted onto robot shells to facilitate complicated local interactions.

Here, we developed Morphobot, a swarm robotic platform for morphogenetic engineering (Fig. 1). To balance the precise motion control and facilitating interactions among robots, we selected DC coreless motors that have precise motion control and needle legs that facilitate interactions. To fulfill the third requirement, the Morphobot includes a robot base and a changeable and functionalized shell. In Section II, we described the hardware design of Morphobot. After that, we demonstrated Morphobot's advantages in morphogenetic engineering in two experiments of morphogenesis in Section III. Finally, we concluded this letter and introduced several morphogenetic engineering projects that are suitable for Morphobot in Section IV.

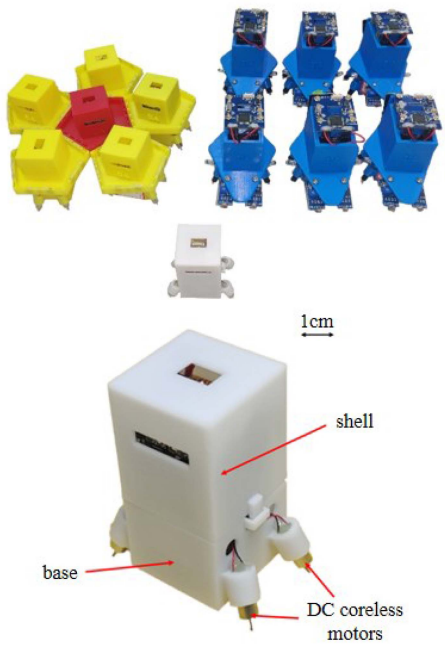

Fig. 1. Morphobots and their several shells.

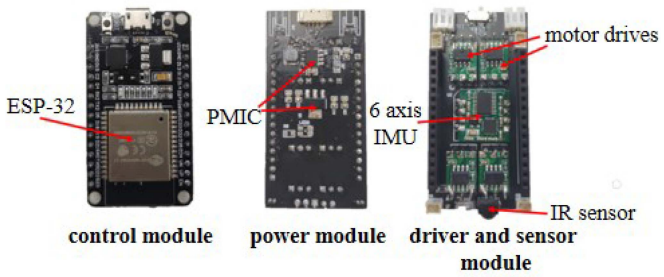

Fig. 2. Circuit boards of morphobot.

II. Hardware Design

The Morphobot is designed specifically for morphogenetic engineering. Besides meeting the three requirements outlined above, Morphobot also has the features of robot swarm platforms in general, including small size, scalability, low cost, and power management.

Morphobot has a footprint of $3.5 \times 3.8\ \text{cm}^2$. It is small enough to conduct experiments on a table and can easily be picked up with one hand. A Morphobot is relatively low cost (∼$35) compared with most existing swarm robots shown in Table I. We described the hardware design in the following subsections.

A. Controller and Programming Platform

The controller of Morphobot is ESP-32 SoC (System-on-Chip), shown in Fig. 2. This SoC has both Wi-Fi and Bluetooth wireless communication modes. It has a dual-core32-bit MCU (Microcontroller Unit) with 16 MB Flash memory and 520 KB SRAM. The main frequency of the dual-core MCU is up to 240 MHz, and computing power is up to 650 DMIPS (Dhrystone Million Instructions Executed Per Second). ESP-32 SoC can be programmed in two ways: using C language on the Arduino IDE (Integrated Development Environment) and using Python on the Thonny IDE. The Arduino community has developed a rich library of functions, which can be easily called when needed. This method is suitable for rapid iterations during development. Meanwhile, the Python on the Thonny IDE offers friendly programming interface and flexibility to write your own functions. These two programming methods facilitate a quick start and enough flexibility.

B. Sensors and Power System

In morphogenic engineering, individual robots interact with their neighbors through both physical interactions and information communications. The individual robots in swarms thus are required to sense their environment and communicate with their neighbors. The Morphobot has infrared sensors at its bottom to communicate with other robots. A Morphobot shoots infrared light on the ground, and the scattered light can be sensed by the IR sensors at the bottom of the surrounding robots. This enables the robot to communicate with its neighbors. Besides infrared sensors, the robot is also mounted with a six-axis attitude sensor, which includes a three-axis accelerometer and a three-axis gyroscope. This sensor detects the robot's attitude information that can form a semi-closed loop control with motion module of the robot.

Because the relationships between the local interactions and global patterns in self-organized systems are implicit, an experiment cannot be interrupted. The Morphobot provides enough power to operate for 1.5 hours, which is enough for most of the experiments.

C. Locomotion

The locomotion module needs to satisfy two characteristics we proposed in the previous section: precise motion control and facilitating interactions among robots. These seemingly contradictory characters are balanced by combining the advantages of two designs in the literature [9], [16]. Four DC coreless motors drive a Morphobot to move. These DC coreless motors are installed onto the robot base at a specific angle relative to the ground, as shown in Fig. 1. The motors maintain a point contact with the ground, so the motion of a Morphobot is easily influenced by its neighbor robots. Furthermore, these DC coreless motors drive the Morphobot via rotation, which provides the robot with strong motion capability. Each Morphobot contacts the ground with only four points. It thus needs to run on a flat surface. Moreover, it would be better to keep all the robots confined to an area with appropriate size, which increases the probabilities of interactions among robots. The driving mechanisms of the four simplest movements are shown in Fig. 3. These movements are moving forward, backward, left, and right. When the first and second motors rotate clockwise, the third and fourth motors rotate counterclockwise, the four forces that ground exert on motors will create a combined forward force and drive the robot moves forward. When the first and third motors rotate counterclockwise, the second and fourth motors rotate clockwise, the four forces that ground exert on motors will create a combined leftward force and drive the robot moves leftward. The other two motions are in a similar manner. The differential driving from four motors can generate more complicated motions of a Morphobot. Some of these patterns of movement will be shown in the experiments in the following section of this letter.

D. Scalability and Shell

Because of the Wi-Fi function of the ESP-32 SoC, each Morphobot can connect to a router in the platform. The server computer serves as EMQX (Elastic Message Queuing Telemetry Transport Broker) platform, and transmits information among all Morphobots in this platform. The number of Morphots on the platform is limited by the router's mount capability. This communication network ensures that Morphobots can be controlled in both centralized and decentralized manners. In swarm robotics, the power supply affects the capability of the platform to test new algorithms. The external power interface of the Morphobot platform allows multiple Morphobots to charge simultaneously. If necessary, the multiple Morphobots can be charged wirelessly at the same time. This is greatly convenient for researchers.

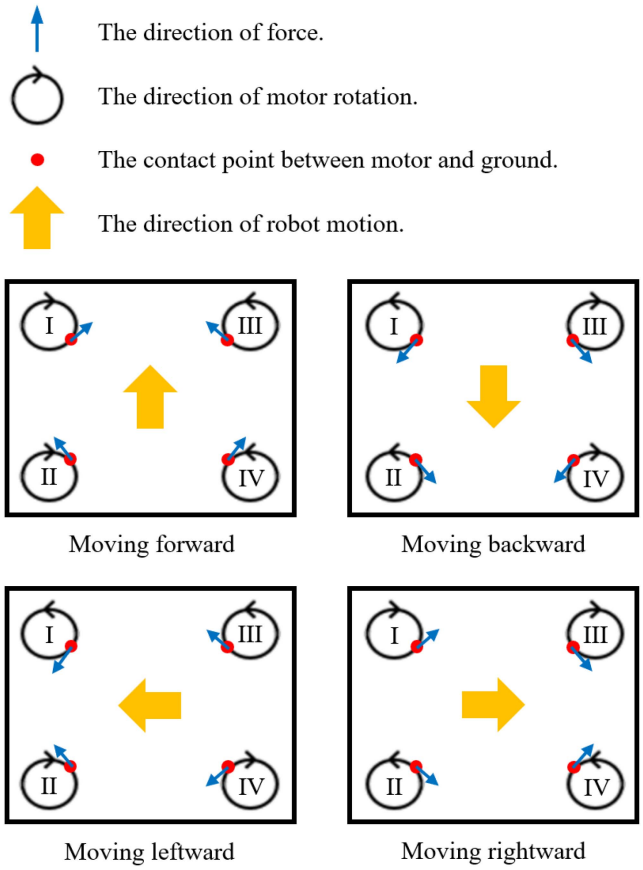

Fig. 3. Morphobot's driving principle.

The changeable and functional shells of a Morphobot allow it to perform different functions during the experiments. The features of shells offer programmable variables in morphogenetic engineering investigations. They can be programmed by geometrical and mechanical features. They can also be coded by integrating electronic circuits. In our third experiment, we used a type of shell that combines geometrical structure with electronic circuits. The electronic circuit retains an interface for serial communication, which expands the computational capability of a Morphobot.

III. Experiments

In this section, we design three different experiments to demonstrate the advantages of Morphobot in morphogenetic engineering research. We first tested the mobility of Morphobots. Next, we design a morphogenesis experiment via physical interactions. Finally, we generated a special morphology, a self-organized dynamic circle, based on optical communication among nearby robots using Morphobots.

A. Testing the Performance of Morphobots

We tested the Morphobots' ability of following linear, circular, and special trajectories respectively. All of the performance tests were done on a table with a size of 76×61 cm^2. A camera was mounted overhead of the table to record the Morphobot's position during the experiments. We analyzed the video data using algorithms in MATLAB.

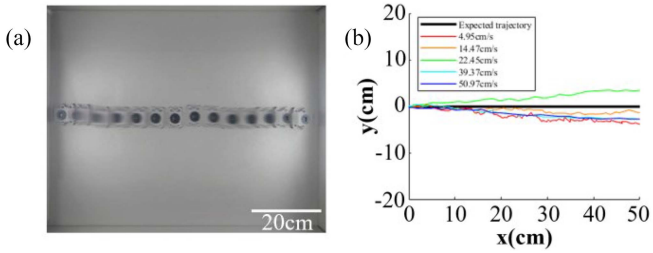

Fig. 4. Linear trajectory experiment. (a) Linear trajectory of one morphobot. (b) Representative trajectories of each velocity.

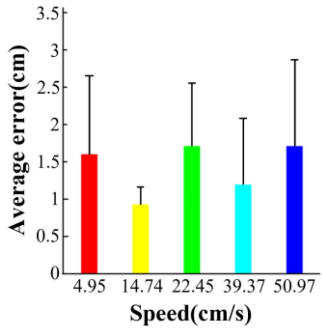

Fig. 5. Average error and standard deviation of ten samples in each velocity.

Fig. 6. Circular trajectory of one morphobot.

We tested the Morphobot's ability to follow a straight line at five different speeds, and took ten samples at each speed. One trajectory of linear sample as shown in Fig. 4(a). We extract the position coordinates of the Morphobot in each frame of the video. The error is defined as the sum of differences between the experimental and the expected trajectory coordinates along the expected trajectory. Fig. 5 shows the average errors and standard deviation in all velocities. The representative trajectories of each velocity are shown in Fig. 4(b), with the expected trajectory shown in black. We found that the Morphobot follows a straight line quite well regardless of its velocity.

Using the same velocities, we test the Morphobot's ability to follow circular trajectories, as a representative trajectory shown in Fig. 6. We show ten groups of trajectories of each speed in yellow lines in Fig. 7, with the expected trajectory shown in black line. As the speed of each Morpnobot increased, the repetition accuracy of Morphobot's circular trajectory got worse. When the speed of each Morphobot is higher than 22.45 cm/s, the Morphobot could not complete a circular trajectory. A faster

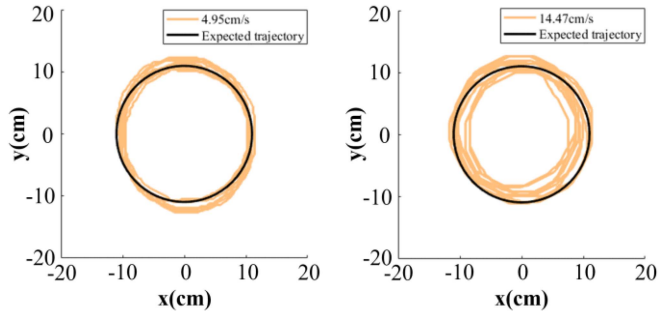

Fig. 7. Ten circular trajectories for each set of speeds.

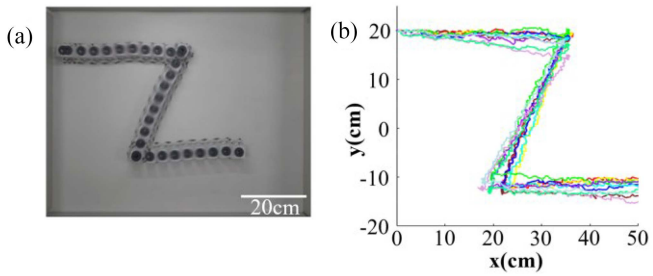

Fig. 8. Z-shaped trajectory experiment. (a) Z-shaped trajectory of one morphobot. (b) Ten Z-shaped trajectories.

circular motion generates a larger centrifugal force. When the centrifugal force is larger than the breakout friction between the Morphobot and ground, the Morphobot cannot maintain a circular trajectory.

Finally, we tested Morphobots following a Z-shaped trajectory, as presented in Fig. 8(a). The robot first moved toward the positive X direction. When it arrives at the first turning point of the "Z", it turned clockwise in place by 120 degrees. After that, the robot moved along its positive direction to the second turning point of the "Z". It then turned counterclockwise in place by 120 degrees. Last, the robot continues to move in the positive X direction to finish the "Z" shape trajectory. In this experiment, all the Morphobots started on a same point of the table. We repeated the Z-shape trajectory experiments ten times. All of these trajectories are shown in a coordinate system, and their Y-coordinates were removed to a suitable position, Fig. 8(b). The results demonstrated that the Morphobot could follow the Z-shaped trajectory well.

B. Morphogenetic Engineering by Physical Interactions Among Morphobots

The DAH (Differential Adhesion Hypothesis) proposed that the differences in intercellular adhesion segregate the different cell types. The low-adhesive cells surround the high-adhesive cells. From the physical perspective, the cells of lower surface tension tend to envelop the cells of higher surface tension [26]. The self-organized cell sorting principle has explained the budding and branching of stratified epithelium in embryo [8]. According to this principle, a robot swarm system can form pre-defined morphology when we properly program the physical

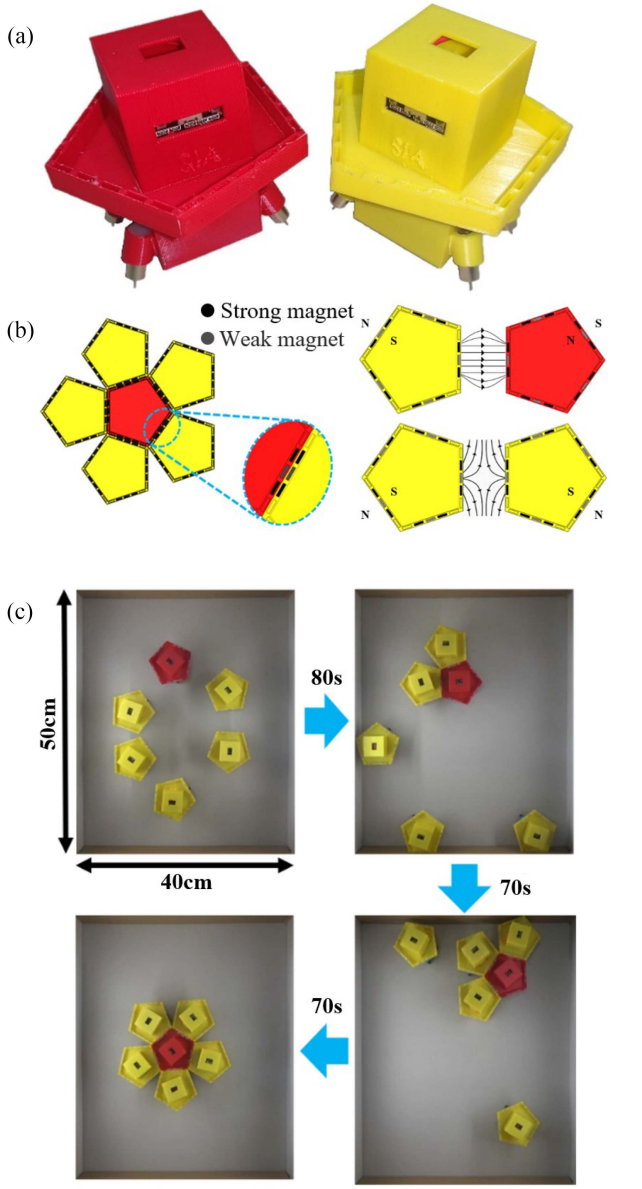

Fig. 9. Physical interactions morphogenetic engineering. (a) Morphobot's red and yellow pentagonal shells. (b) Principles of physical morphogenesis. (c) Physical morphology of "sunflower" forming.

interaction. In this letter, the robots interacted with each other via magnetic forces between their shells. There are two types of pentagonal shells we designed for the Morphobot swarm, red ones and yellow ones in Fig. 9(a). Each side of the pentagon has five rectangular slots for cylindrical magnets. In this experiment, we used six Morphobots, a red one and five yellow ones. By assigning the cylindrical magnets into the slots in the shell properly, the Morphobot swarm eventually formed a "sunflower" morphology. This experiment was done on a 40 $\times$ 50 cm^2 table with an overhead camera for recording the movement of Morphobots.

On each side of a pentagonal shell, we put cylindrical magnets in rectangular slots. By analyzing the components of the predesigned morphology of "sunflower", we assigned the five

Morphobot with yellow shells surrounding the red Morphobot. In Morphobot with red shell, the S-pole of cylindrical magnet faced outward. The N-pole of cylindrical magnets faced outward in Morphobots with yellow shells, as presented in Fig. 9(b). In this way, the red shell attracted the yellow shell and the two yellow shells repelled each other. In order to make the sides of each two pentagons mesh perfectly, we only placed magnets in three rectangular slots at the middle of each side of the shell. A weak magnet was placed in the middle slot. Two strong magnets were placed at the other two adjacent slots. Throughout the experiment, the robot moved straight forward and followed a rotation to avoid getting stuck at the corner of the stage. This moving mode could be viewed as pseudo-random moving.

Fig. 9(c) shows images of the process of experiments. Initially, six Morphobots were randomly placed on the table. The experiment ended when the five Morphobots with yellow shells perfectly combined with the Morphobot with red shell, shown in the supplemental video. The whole experiment took about 220 seconds.

C. Morphogenetic Engineering by Informational Communication Among Morphobots

A large school of fish coherently swims in a clockwise or counterclockwise circular formation to evade predators. This phenomenon is termed milling [27], [28]. Gauci et al. [29], [30] proposed a simple binary algorithm, which allows robot swarms self-organized aggregation without computation. Based on this algorithm, Berlinger et al. [31] developed a milling morphology of fish-inspired robots' swarm. The individual fish-inspired robot of swarms performs different movements in the presence or absence of other individuals within their field of view. It has been verified that this algorithm could also form circling of ground robot swarm in simulation. Here, we designed a shell for Morphobots to form this morphology on the ground experimentally, Fig. 10(a). Because this morphology is formed through communication between robots, we call it communication morphogenesis. The shell we designed for this experiment has two light sensors in the front, which return low voltage when they sense light. LEDs emitting white light are installed on the left, right, and back of the shell. At the top of the shell is a 51 MCU control board that communicates with Morphobot by serial port. All light sensors and LEDs are controlled by the 51 MCU control board.

In this experiment, each Morphobot follows the same control algorithm. This control algorithm is that the robot rotates in a clockwise direction and the three led lights remain on. When the light sensors detect light, the Morphobot rotates counterclockwise, Fig. 10(b).

All communication morphogenesis experiments were done on a 120 $\times$ 120 cm^2 table. We installed a video camera overhead of the table to record the whole motion process. Because we use light sensors, the experiment needs to be done in the dark. Fig. 11(a) shows that we use four, five, and six Morphobots to form the morphology. The red dotted circle means the size of the morphology formed by Morphobots at that time. With the swarm of four Morphobots, it was quite often that one

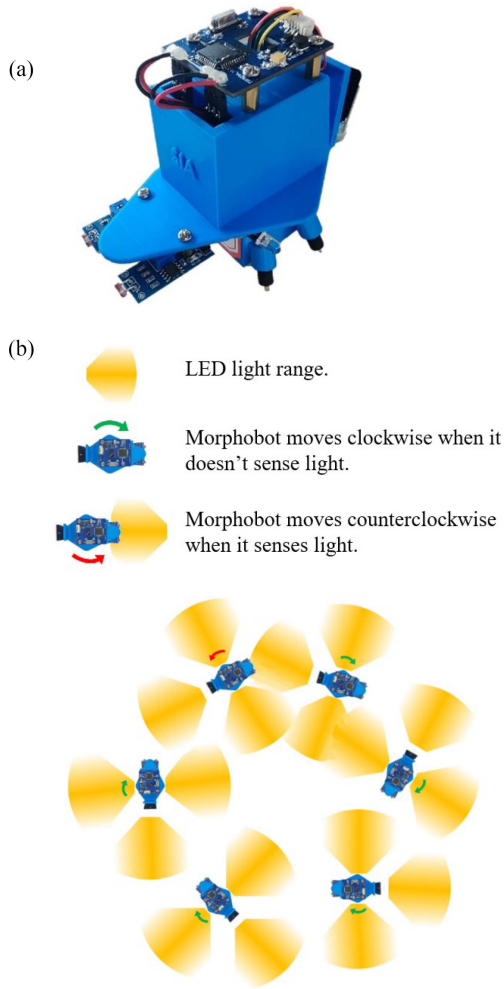

Fig. 10. Informational communication morphogenetic engineering. (a) Morphobot's communication morphogenesis shell. (b) Principles of communication morphogenesis.

robot ran out of the circle. After five robots formed a stable-circling morphology, we tested the effect of adding or removing one robot from the swarm. We found that this morphology would still be formed after adding or removing a robot, but the size would be changed, as shown in Fig. 11(a) and the supplemental video.

We extracted the motion trajectories of Morphobots in this experiment, presented in Fig. 11(b). In each set of experiments, the trajectories of different robots are presented in different colors. The results suggested that the more Morphobots in a swarm, the better roundness of the circling morphology. We calculated the distance of each robot from the center of the circle at every moment, as presented in Fig. 11(c). The lines with the same color in Fig. 11(b) and (c) represent the trajectory of the same robot. The range of the data in swarm of 4 robots was much larger than that of the swarms of 5 and 6 robots respectively.

Using the data between 7 and 14 seconds, we calculated their mean and standard deviation, as presented in Fig. 12. We find that the mean radius is larger in the experiment with more Morphobots, which is consistent with the previous report in school

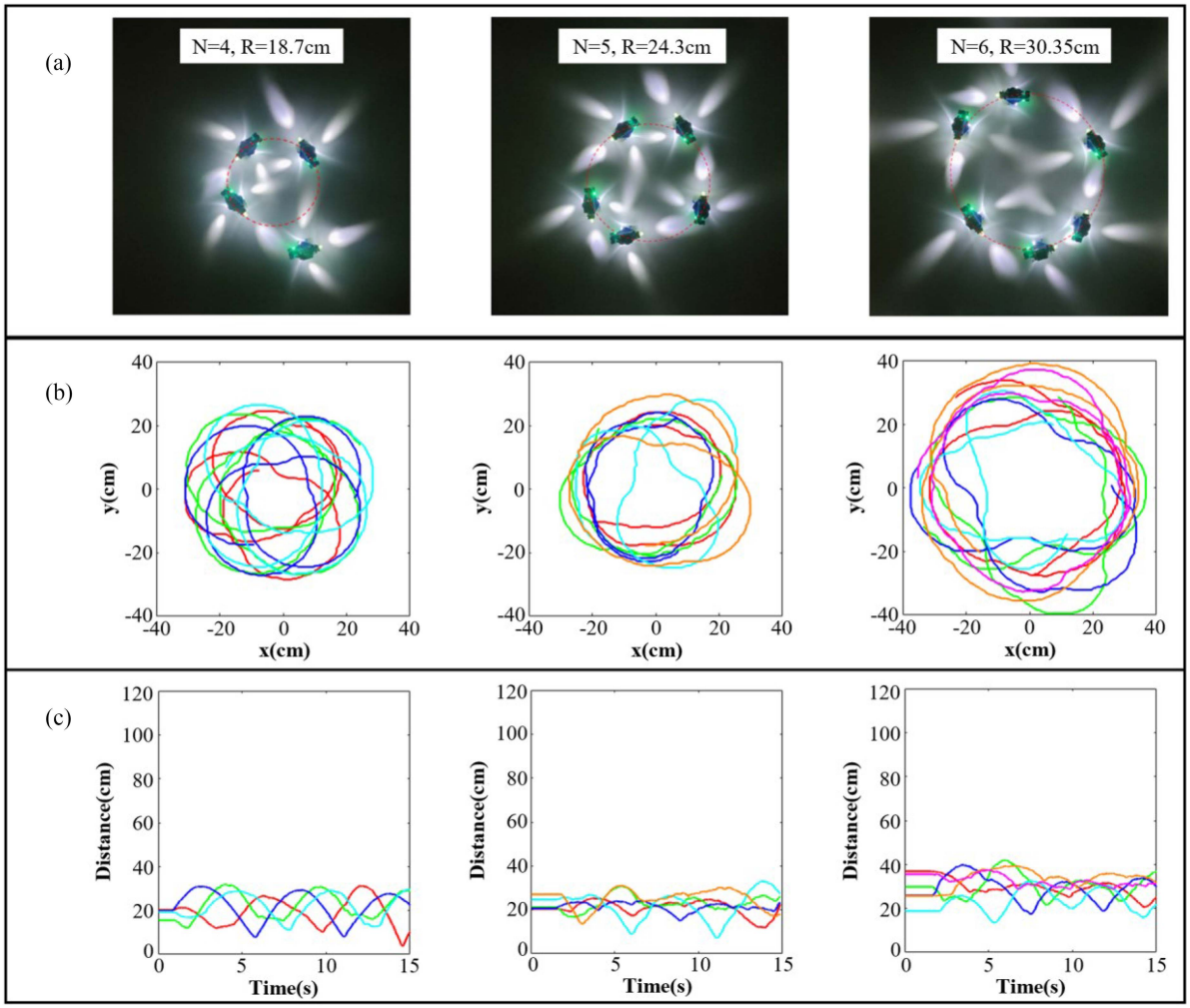

Fig. 11. Communication morphogenesis experiments. (a) Morphology formed by three quantities of morphobots. (b) Trajectories of communication morphogenesis experiment. (c) Distance of each robot from the center.

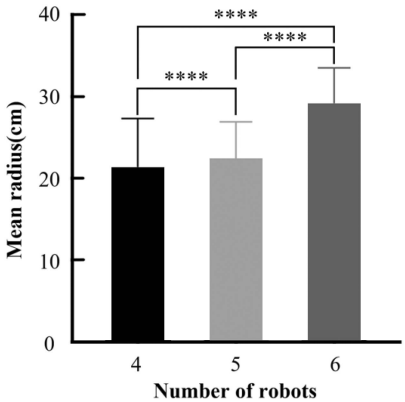

Fig. 12. Mean radius and standard deviation of each set. Statistics: ****, t-test $p < 0.0001$.

of fish-inspired robots [31]. The standard deviation, however, is smaller within experiments with more Morphobots. It suggested that a swarm of more Morphobots might be circling with a better roundness. This is consistent with the results presented in Fig. 11(b) and (c). This is an interesting phenomenon that deserves a comprehensive investigation.

IV. Conclusion

We present the Morphbot specifically designed for morphogenetic engineering. Besides meeting the requirements of scalability, such as small size and low cost, Morphobot also fulfills the three characteristics of morphogenetic engineering. We introduced the design of Morphobot and characterized its performance. After these, we executed two experiments of morphogenesis. They proved that Morphobot could be used in morphogenesis through physical interactions and communications. In the future, we will package the components of Morphobot into ROS simulation environment. In this way, we can integrate simulation and experiment studies in the same platform. This will offer a powerful tool for the field of morphogenetic engineering.

Acknowledgment

The authors would like to thank Shen Tian and Hongwei Wang for their help in designing the Morphobot.

REFERENCES

[1] W. Wang, Y. Zheng, G. Lin, L. Zhang, and Z. Han, "Swarm robotics: A review," *Robot*, vol. 42, no. 2, pp. 232–256, 2020.

[2] Z. Kashino, J. Y. Kim, G. Nejat, and B. Benhabib, "Spatiotemporal adaptive optimization of a static-sensor network via a non-parametric estimation of target location likelihood," *IEEE Sensors J.*, vol. 17, no. 5, pp. 1479–1492, Mar. 2017.

[3] D. Roy, M. Maitra, and S. Bhattacharya, "Exploration of multiple unknown areas by swarm of robots utilizing virtual-region-based splitting and merging technique," *IEEE Trans. Automat. Sci. Eng.*, vol. 19, no. 4, pp. 3459–3470, Oct. 2022.

[4] M. Rosalie et al., "Area exploration with a swarm of UAVs combining deterministic chaotic ant colony mobility with position MPC," in *Proc. Int. Conf. Unmanned Aircr. Syst.*, 2017, pp. 1392–1397.

[5] A. Breitenmoser, M. Schwager, J.-C. Metzger, R. Siegwart, and D. Rus, "Voronoi coverage of non-convex environments with a group of networked robots," in *Proc. IEEE Int. Conf. Robot. Automat.*, 2010, pp. 4982–4989.

[6] K. N. McGuire, C. De Wagter, K. Tuyls, H. J. Kappen, and G. C. H. E. De Croon, "Minimal navigation solution for a swarm of tiny flying robots to explore an unknown environment," *Sci. Robot.*, vol. 4, no. 35, Oct. 2019, Art. no. eaaw9710.

[7] I. Slavkov et al., "Morphogenesis in robot swarms," *Sci. Robot.*, vol. 3, no. 25, Dec. 2018, Art. no. eaau9178.

[8] S. Wang, K. Matsumoto, S. Lish, A. Cartagena-Rivera, and K. Yamada, "Budding epithelial morphogenesis driven by cell-matrix versus cell-cell adhesion," *Cell*, vol. 184, no. 14, pp. 3702–3716, Jul. 2021.

[9] M. Rubenstein, C. Ahler, N. Hoff, A. Cabrera, and R. Nagpal, "Kilobot: A low cost robot with scalable operations designed for collective behaviors," *Robot. Auton. Syst.*, vol. 62, no. 7, pp. 966–975, Jul. 2014.

[10] D. Pickem, M. Lee, and M. Egerstedt, "The GRITSBot in its natural habitat-a multi-robot testbed," in *Proc. IEEE Int. Conf. Robot. Automat.*, 2015, pp. 4062–4067.

[11] S. Kernbach, R. Thenius, O. Kernbach, and T. Schmickl, "Re-embodiment of honeybee aggregation behavior in an artificial micro-robotic system," *Adaptive Behav.*, vol. 17, no. 3, pp. 237–259, Jun. 2009.

[12] G. Caprari and R. Siegwart, "Mobile micro-robots ready to use: Alice," in *Proc. IEEE/RSJ Int. Conf. Intell. Robots Syst.*, 2005, pp. 3295–3300.

[13] G. Caprari, T. Estier, and R. Y. Siegwart, "Fascination of down scaling–Alice the sugar cube robot," *J. Micromechatronics*, vol. 1, no. 3, pp. 177–189, 2000.

[14] F. Mondada et al., "The e-puck, a robot designed for education in engineering," in *Proc. 9th Conf. Auton. Robot Syst. Competitions*, 2009, vol. 1, pp. 59–65.

[15] C. Hu, Q. Fu, and S. Yue, "Colias IV: The affordable micro robot platform with bio-inspired vision," in *Towards Autonomous Robotic Systems*, M. Giuliani, T. Assaf, and M. E. Giannaccini, Eds. Berlin, Germany: Springer, 2018, pp. 197–208.

[16] K. Eshaghi, Y. Li, Z. Kashino, G. Nejat, and B. Benhabib, "*mROBerTO 2.0*–An autonomous millirobot with enhanced locomotion for swarm robotics," *IEEE Robot. Automat. Lett.*, vol. 5, no. 2, pp. 962–969, Apr. 2020.

[17] A. P. Sabelhaus, D. Mirsky, L. M. Hill, N. C. Martins, and S. Bergbreiter, "TinyTeRP: A tiny terrestrial robotic platform with modular sensing," in *Proc. IEEE Int. Conf. Robot. Automat.*, 2013, pp. 2600–2605.

[18] F. Arvin, K. Samsudin, and A. R. Ramli, "Development of a miniature robot for swarm robotic application," *Int. J. Comput. Elect. Eng.*, vol. 1, no. 4, pp. 436–442, 2009.

[19] H. Oh, A. Shiraz, and Y. Jin, "Morphogen diffusion algorithms for tracking and herding using a swarm of kilobots," *Soft Comput.*, vol. 22, no. 6, pp. 1833–1844, Mar. 2018.

[20] J. McLurkin et al., "A low-cost multi-robot system for research, teaching, and outreach," in *Proc. Distrib. Auton. Robotic Syst.: 10th Int. Symp.*, 2010, pp. 597–609.

[21] J. McLurkin, J. Smith, J. Frankel, D. Sotkowitz, D. Blau, and B. Schmidt, "Speaking Swarmish: Human-robot interface design for large Swarms of autonomous mobile robots," in *Proc. Assoc. Adv. Artif. Intell. Spring Symp.*, 2006, pp. 72–75.

[22] S. Wilson et al., "Pheeno, a versatile swarm robotic research and education platform," *IEEE Robot. Automat. Lett.*, vol. 1, no. 2, pp. 884–891, Jul. 2016.

[23] J. Betthauser et al., "WolfBot: A distributed mobile sensing platform for research and education," in *Proc. Zone 1 Conf. Amer. Soc. Eng. Educ.*, 2014, pp. 1–8.

[24] M. Bonani et al., "The marXbot, a miniature mobile robot opening new perspectives for the collective-robotic research," in *Proc. IEEE/RSJ Int. Conf. Intell. Robots Syst.*, 2010, pp. 4187–4193.

[25] M. Dorigo, "SWARM-BOT: An experiment in swarm robotics," in *Proc. IEEE Swarm Intell. Symp.*, 2005, pp. 192–200.

[26] R. Foty and M. Steinberg, "The differential adhesion hypothesis: A direct evaluation," *Devlop. Biol.*, vol. 278, no. 1, pp. 255–263, Feb. 2005.

[27] B. Partridge, "The structure and function of fish schools," *Sci. Amer.*, vol. 246, no. 6, pp. 114–123, 1982.

[28] J. Parrish, S. Viscido, and D. Grunbaum, "Self-organized fish schools: An examination of emergent properties," *Biol. Bull.*, vol. 202, no. 3, pp. 296–305, Jun. 2002.

[29] M. Gauci, J. Chen, T. Dodd, and R. Gross, "Evolving aggregation behaviors in multi-robot systems with binary sensors," in *Distributed Autonomous Robotic Systems*, M. Hsieh and G. Chirikjian, Eds. Berlin, Germany: Springer, 2014, pp. 355–367.

[30] M. Gauci, J. Chen, W. Li, T. Dodd, and R. Gross, "Self-organized aggregation without computation," *Int. J. Robot. Res.*, vol. 33, no. 8, pp. 1145–1161, Jul. 2014.

[31] F. Berlinger, M. Gauci, and R. Nagpal, "Implicit coordination for 3D underwater collective behaviors in a fish-inspired robot swarm," *Sci. Robot.*, vol. 6, no. 50, Jan. 2021, Art. no. eabd8668.